

# Interlaminar modelling to predict composite coiled tube failure



Lead author  
**Siamak  
Mishani**

**S. Mishani<sup>1</sup>, B. Evans<sup>1</sup>, V. Rasouli<sup>1</sup>, R. Roufail<sup>1</sup>, S. Soe<sup>2</sup>  
and P. Jaensch<sup>2</sup>**

<sup>1</sup>Deep Exploration Technologies Cooperative Research Centre (DET CRC)

Department of Petroleum Engineering, Curtin University  
26 Dick Perry Avenue  
Kensington, WA 6151

<sup>2</sup>DET CRC

Burbridge Business Park  
26 Butler Boulevard  
Adelaide Airport, SA 5950  
Siamak.Mishani@yahoo.com

## ABSTRACT

In a field operation that uses coiled tubing in its applications, fibre-reinforced polymer matrix composite tubing is seldom used. Fibre-composite coiled tubes offer advantages, compared to steel material, through a reduction in weight and improvement in fatigue life.

The stiffness of composite material degrades progressively when increasing the number of cyclic loading. The fatigue damage and failure criteria of fibre-reinforced composite coiled tubes are more complex than that of steel; hence, failure predictions are somewhat unreliable.

Among the defects in composite materials, interlaminar delamination is the foremost problem in fibre-reinforced composite material, and it leads to a reduction in strength and stiffness especially in cyclic-load conditions. Delamination causes a redistribution of the load path along the composite structure, which is unpredictable; therefore, delamination in a composite coiled tube in an oil and gas field eventually leads to final failure, which could be catastrophic.

A-ply-by-ply mathematical modelling and numerical simulation method was developed to predict interlaminar delamination of filament-wound composite coiled tubes under a combination of different loading scenarios with consideration to low-cycle fatigue.

The objective of this paper is to explain interlaminar delamination as an initial crack and source of stress concentration in composite coiled tubes in the framework of meso-cracking progression of matrix damage modelling of composite laminates.

The paper focuses on delamination failure because the largest span of the composite lifecycle is at the crack propagation phase, which manifests itself in the form of delamination. The analysis shows that the crack front tip is not uniform, and also shows that carbon fibre possesses higher stiffness values compared to glass fibre. The paper confirms that 2D modelling cannot express the real release strain energy rate at the crack front tip. Mode-I testing, however, showed that the double cantilever beam (DCB) only represents the normal stress from the release strain energy rate. The results also indicated that there were other sources contributing to the strain energy release rate, such as inter-layer frictions and normal stress in the end notched flexure (ENF) testing mode.

## KEYWORDS

Coiled tubing, delamination, damage, stiffness, fibre composites, fatigue, modelling.

## INTRODUCTION

Coiled tubes are under different loading conditions, and cyclic bending and straightening during running in and pulling out of wellbores. Reifsnider et al (1983) concluded that the damage index value of composite material follows a non-linear graph for cyclic loading (as shown in Fig. 1). During the period of fatigue life many modes of damage—including matrix cracks, interfacial de-bonding, interlaminar failure (delamination) and fibre breakage—can be observed in composite materials (Ochoa and Reddy, 1992).

Delamination is a common failure mode that causes an unpredictable redistribution of the load path along the composite structure and leads to a reduction in the strength and stiffness of the fibre-reinforced composite material (Szekrenyes, 2002). Although delamination occupies the highest percentage of the middle period of the fatigue life, the changes in the damage index are not available; as a result, the investigation of crack propagation between the layers is unclear and, consequently, composite materials often need to be over-designed with an additional margin of safety to compensate for the deficiency in predicting its lifetime in cyclic-load conditions (Degrieck and Van Paepegem, 2001).

The damage index, as a physical parameter that quantifies the degradation of composite material (Gibson, 2011), can be calculated using Equation 1 according to Wu and Yao (2010).

$$D_n = \frac{E_0 - E_n}{E_0 - E_f} \quad (1)$$

Refer to the nomenclature section of this paper for definitions of each variable.

According to Figure 1, when the crack density saturation (CDS) occurs in the matrix, the tip of the delamination initiates and propagates. Based on the meso-scale damage model, therefore, a composite laminate is defined as a stacking sequence (Jones, 1998) of elementary composite layers and interfaces (Fig. 2) with different mechanical properties. The meso-scale damage model helps to define the interlaminar delamination phenomenon as interface cracking or loss of cohesion between layers (Burlayenko and Sadowski, 2008).

Delamination (inter-ply damage) growth causes a reduction of the load capacity by both tensile and shear stresses at the delaminated interface, which would eventually cause failure to the laminate composite structure (Szekrenyes, 2002). Tensile and shear stresses in the pre-existing delaminated layer can be measured by Mode-I and Mode-II interlaminar fracture toughness testing methods, respectively. The interlaminar fracture toughness of composite material can be quantified by the strain energy release rate ( $G_i$ ) in

Mode-I testing for pure normal stress, ( $G_{II}$ ) in Mode-II testing for pure shear stress, and ( $G_{III}$ ) for pure sliding stress. As shown in Equation 2, the total strain energy release rate ( $G_T$ ) expresses the total pure strain energy release rates from normal, shear and sliding stresses. Interlaminar fracture toughness shows the resistance of composite materials to delamination (Thakur, 2013); therefore, it is an important composite property and widely acknowledged by designers.

$$G_T = G_I + G_{II} + G_{III} \quad (2)$$

Ply-by-ply mathematical modelling and numerical simulations were developed to predict interlaminar delamination of filament-wound composite coiled tubes. Fracture test models such as the double cantilever beam (DCB) and end-notched flexure (ENF) models can be used to extract fracture parameters.

Three-dimensional commercial finite element software—ANSYS/APDL version 15.0—was used for all simulations. The virtual crack closure technique (VCCT) and cohesive zone model (CZM) were used to determine delamination growth in an initially delaminated composite model. The finite element model was evaluated under a combination of different loading scenarios. A comparison between the crack propagation in glass- and carbon-fibre in composite material was then performed.

### Hashin’s failure criteria for unidirectional fibre composites

One of the critical problems in the design and modelling of fibre-reinforced composite material under cyclic loading is to establish meaningful fatigue failure criteria. There are many failure criteria for the design and modelling of composite material (Barbero, 2013).

Hashin (1980) proposed a failure criterion for unidirectional fibre-composite materials based on quadratic stress polynomials. Hashin’s failure criteria indicated that there are

two independent failure modes in unidirectional fibre composites: fibre failure and inter-fibre failure. In the fibre failure mode, composite material fails due to a rupture resulting from a tension force and buckling from a compressional force. Matrix (inter-fibre) failure occurs in a plane parallel to the fibres (Hashin, 1980).

Unidirectional fibre composites are transversely isotropic in the fibre direction; therefore, fibre-reinforced failure modes consider the uni-axial stress state in the fibre direction, while matrix failure modes consider the tri-axial stress state.

Hashin’s failure criteria involved four failure modes for fibres and matrices (Hashin, 1980):

1. tensile fibre failure for  $\sigma_{11} \geq 0$ ;
2. compressive fibre failure for  $\sigma_{11} < 0$ ;
3. tensile matrix failure for  $\sigma_{22} + \sigma_{33} \geq 0$ ; and,
4. compressive matrix failure for  $\sigma_{22} + \sigma_{33} < 0$ .

### Interlaminar fracture (delamination)

Three crack propagation failure modes of delamination are shown in Figure 3 for interlaminar crack displacements. The numerical simulation of the crack propagation follows two procedures. The first is based on fracture mechanics, and the second is based on a mixture of damage mechanics and softening plasticity (Spada et al, 2009).

The mechanical parameters indicate that delamination happens through the interface layer. The resistance of the interface to propagate the interlaminar crack under the opening mode (Mode-I) is different from under the shear mode (Mode-II). The increase of force applied in Mode-I and Mode-II gives rise to tensile and shear stresses at the delamination crack front, respectively (Mathews and Swanson, 2007).

A delamination crack propagates when the strain energy release rate is equal to or greater than the value of the critical energy release rate (Alfano and Crisfield, 2001).

### Crack opening mode (Mode-I)

According to Wisheart and Richardson (1998), the strain energy release rate can be statically measured using a DCB test for Mode-I delamination. The model is designed with a pre-existing crack. By applying an opposite direction force to the end of the sample, perpendicular to the crack surface, the pre-existing crack will extend. Figure 4 shows the crack geometry, the reaction forces and crack displacements. The reaction forces are calculated according to Equation 3 and the resultant crack displacements are used to calculate the total fracture toughness energy ( $G_I$ ). A schematic diagram of the DCB is shown in Figure 5.

$$G_I = \frac{1}{2} \frac{R_y}{da} dv \quad (3)$$

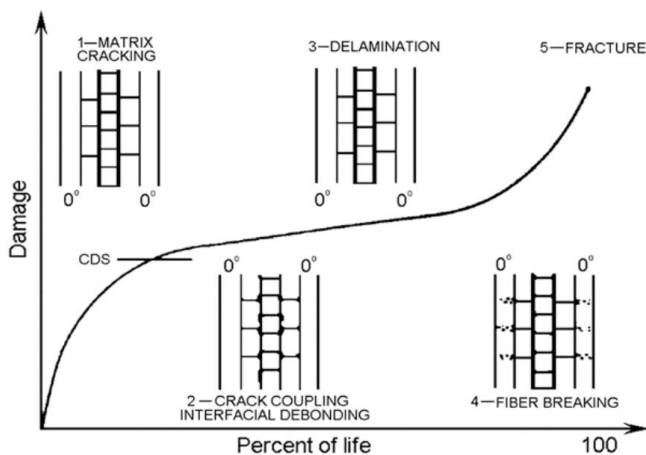


Figure 1. Damage index in composite material (Reifsnider et al, 1983).

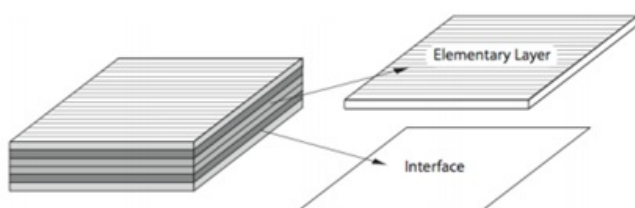


Figure 2. Meso-scale damage model of a laminate (Bordeu and Boucard, 2009).

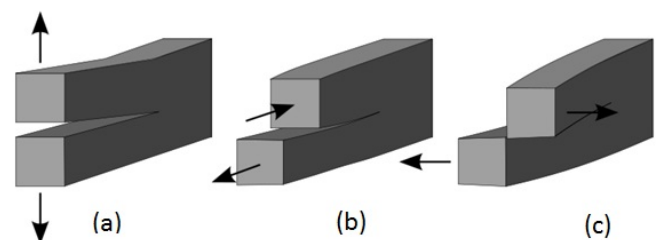


Figure 3. Crack growth modes: (a) opening Mode-I; (b) sliding shear Mode-II; and, (c) scissoring shear Mode-III (Van Mier, 2012).

## DCB (Mode-I)

The crack opening mode (Mode-I) test is generally performed on a unidirectional composite laminate specimen. In this method, the applied load versus crack displacement is linear, and the first deviation from linearity occurs as the crack initiation happens. According to fracture mechanics concepts, the propagation from a pre-existing delamination can be calculated by the amount of strain energy release rate and the fracture toughness of the interface (Choupani, 2008).

The interlaminar fracture toughness calculations are based on Equation 4 (Prasad et al, 2011).

$$G_I = \frac{3 P \delta}{2 b a} \quad (4)$$

## Crack sliding mode (Mode-II)

Mode-II delamination failure is a method for measuring shear stresses at the crack tip. A three-point bending load on the ENF specimen with a pre-existing crack ( $a$ , as shown in Fig. 6) can determine the strain elastic release energy rate. The pre-existing crack propagates as the bending load is applied to the specimen. The finite element model was designed to simulate a sample similar to the set up shown in Figure 6. According to Equation 5, the total fracture toughness energy ( $G_{II}$ ) is calculated from the reaction force at the crack tip, load point displacement and the crack propagation length.

$$G_{II} = \frac{1}{2} \frac{R_x du}{da} \quad (5)$$

## ENF (Mode-II)

The ENF test is a method for measuring interlaminar fracture toughness in composite materials under in-plane shear stress. The crack sliding mode (Mode-II) is a type of fracture testing method in which the crack initiation and propagation's front faces slide on each other in the direction of the crack's growth path and no crack opening mode occurs (Salehizadeh and Saka, 1992). Mode-II interlaminar fracture toughness is calculated according to Equation 6 and is denoted by  $G_{II}$  (Zhu, 2009).

$$G_{II} = \frac{9 P^2 a^2}{16 E_{11} b^2 h^3} \quad (6)$$

Finite element modelling analysis can use the virtual crack technique and/or cohesive crack model method to compute the strain energy release rate.

## Virtual crack closure technique (VCCT)

The VCCT is a fracture mechanics method that is commonly used for modelling interlaminar delamination failure. The VCCT requires an initial crack in the structure between two layers to model the crack propagation. VCCT computes the strain energy release rate for crack growth. Delamination failure occurs when the strain energy release rate becomes equal to or greater than the critical energy release rate (Sun et al, 2009).

## Cohesive zone model (CZM)

The CZM is based on strength criteria and fracture mechanics concepts. It incorporates the initiation and propagation of

a crack front; however, it cannot predict the initiation of the interlaminar crack. Mesh size and material parameters are important factors in CZM modelling. The interface between the adjacent layers of the composite structure is properly defined to determine the crack propagation. The CZM is considered to be a tool to evaluate the deterioration of cohesion between the layers, which uses the relationship between the separation and traction along the interface. Table 1 shows the strengths and weaknesses of the CZM and CVVT modelling methods.

## Interface

The laminated interface is a 3D medium and its thickness is negligible compared to the laminated specimen dimensions; therefore, modelling the interface layer is defined as a 2D entity to evaluate the relative displacement and reaction force from one layer to the next. Due to low-strength bonding between the adjacent layers, the interface offers the best path for the crack to propagate. The interface strength only depends on matrix properties.

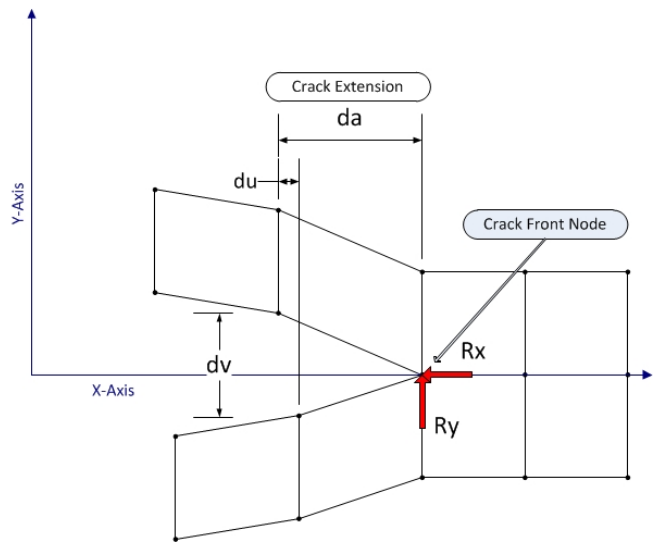


Figure 4. 2D crack geometry of the DCB (Krueger, 2004).

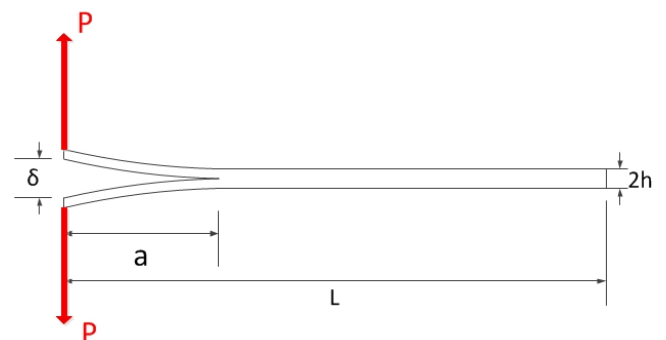


Figure 5. A schematic of the DCB specimen.

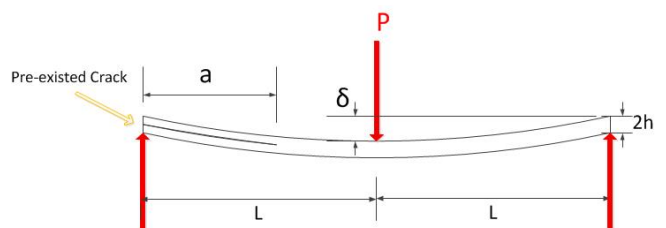


Figure 6. A schematic of the ENF specimen.

## FINITE ELEMENT MODELLING

To study the effect of crack initiation and propagation behavior, a glass-fibre composite material and a carbon-fibre composite material were modelled. The two approaches, VCCT and CZM, were implemented in the finite element analysis software (ANSYS/APDL version 15). The applied load modes evaluated were opening Mode-I using the DCB design according to ASTM D5528, and shear Mode-II using the ENF design according to JIS K7086 standards. The strain energy release rates— $G_I$  and  $G_{II}$ —due to normal and shear stresses, respectively, were evaluated.

### FINITE ELEMENT MODEL

The mechanical properties of the unidirectional composite glass fibre/epoxy, carbon fibre/epoxy and interface epoxy resin are presented in Table 2.

The structure modelled a rectangular cross-section 150 mm long, 25 mm wide and 3 mm high. The pre-existing crack length was 50 mm, as listed in Table 3.

Static analysis is performed using regular mesh eight-node Brick elements with SOLID185 for both DCB and ENF laminates and interlaminar layers.

**Table 1.** Comparison between the CZM and CVVT (ANSYS®, 2013).

	CZM	VCCT
<b>Strengths</b>	<ul style="list-style-type: none"> <li>Prediction of initial and growth of crack.</li> <li>Applicable to complex structures.</li> </ul>	<ul style="list-style-type: none"> <li>Based on fracture mechanics concept.</li> <li>Crack growth related to strain energy release rate.</li> </ul>
<b>Weaknesses</b>	<ul style="list-style-type: none"> <li>Difficult to obtain characterisation data.</li> <li>Accurate assessments are strongly tied to element size.</li> </ul>	<ul style="list-style-type: none"> <li>Necessary to assume number, location and size of the cracks.</li> <li>Difficult to incorporate with complex structures.</li> </ul>

**Table 2.** Mechanical properties.

Material properties	Direction	Glass fibre/ epoxy	Carbon fibre/ epoxy
Young's modulus	X	135.3 GPa	40 GPa
	Y	9 GPa	5 GPa
	Z	9 GPa	5 GPa
Poisson's ratio	XY	0.24	0.27
	YZ	0.46	0.27
	XZ	0.24	0.275
Shear modulus	XY	5.2 GPa	1.07 GPa
	YZ	3.08 GPa	0.806 GPa
	XZ	5.2 GPa	1.07 GPa
Interface		Minimum stress = 25 Mpa	
		Normal separation = 0.004 mm	
		Shear separation = 1,000 mm	

**Table 3.** Modelled sample Dimensions.

Specimen dimensions	Length = 150 mm
	Crack length = 50 mm
	Height = 3 mm
	Width = 25 mm
	Maximum load displacement = 10 mm

To simulate Mode-I (the opening mode), one end of the DCB structure was fixed. The opposite free end (with the pre-existing crack) was subjected to a total of 20 mm of displacement, as shown in Figure 5. For Mode-II (the sliding shear mode), a three-point loading was simulated, similar to the ENF model. Both ends of the sample were supported on one side, and on the opposite side to the sample a 10 mm displacement was exerted through the point load at the centre, as illustrated in Figure 6. The 3D zero thickness interfaces were modelled as an inter-layer cohesive element between the laminate to direct the interlaminar crack propagation front paths.

## RESULTS AND DISCUSSION

A DCB was used to determine Mode-I interlaminar fracture toughness, and the ENF beam was used to determine Mode-II interlaminar fracture toughness. The finite element 3D models are shown in Figure 7 for ENF and DCB. The models illustrate the von-Mises stress distribution in both the ENF and DCB models. According to Equations 2 and 3, the resultant stresses represent the reaction forces, and consequently the energy release rates  $G_I$  for the DCB and  $G_{II}$  for the ENF models were calculated.

Figure 8 shows a contour plot for the crack front face versus total strain energy release rate ( $G_T$ ) for the DCB model in both carbon- and glass-fibre composite laminates. The  $G_I$  and  $G_T$  values are equal at the crack front face for both the carbon- and glass-fibre composite materials. The graphs illustrate that the release energy rate by the carbon fibre was almost three times more than that for the glass-fibre. The results of the Mode-I testing method confirm that the DCB model represents only the pure normal stress from the release strain energy rate  $G_I$  (Brunner et al, 2008).

As presented in Figure 9, the total energy release rate ( $G_T$ ) and shear energy release rate ( $G_{II}$ ) obtained from the ENF model correspond to a crack initiation during the application of slide shear load, Mode-II. The results show that the  $G_T$  values are slightly more than the  $G_{II}$  values (almost 2.5% and 1% at the edges for glass fibre and carbon fibre, respectively). The narrow difference between  $G_T$  and  $G_{II}$  indicates that, apart from shear stress (the evaluation of which was based on the strain energy release rate Mode-II), there are other sources contributing to the strain energy release rate (such as inter-layer frictions and normal stress) in the ENF testing mode. The result confirms Brunner et al's (2008) suggestion that the ENF testing method cannot represent pure shear stress in delamination crack testing.

### Effect of load force on testing approach

The results from the analyses of the load point displacement responses of the applied force to the ENF and DCB models for the carbon- and glass-fibre composite materials are shown in Figures 10 and 11. The contour plots present a meaningful relationship between carbon fibre and glass fibre in Mode-I and Mode-II modelling. In the Mode-I DCB model, for a 10 mm load point displacement, the applied force to the pre-existing crack edges of the model for carbon- and glass-fibre composites are 20 N and 5.6 N, respectively. A 10 mm load point displacement to the center of Mode-II ENF model illustrates 1,500 N for carbon fibre and 470 N for glass fibre. This means that the applied load for the same load displacement in carbon fibre is almost three times more than that of glass fibre in the DCB and ENF models.

*Continued next page.*

Continued from previous page.

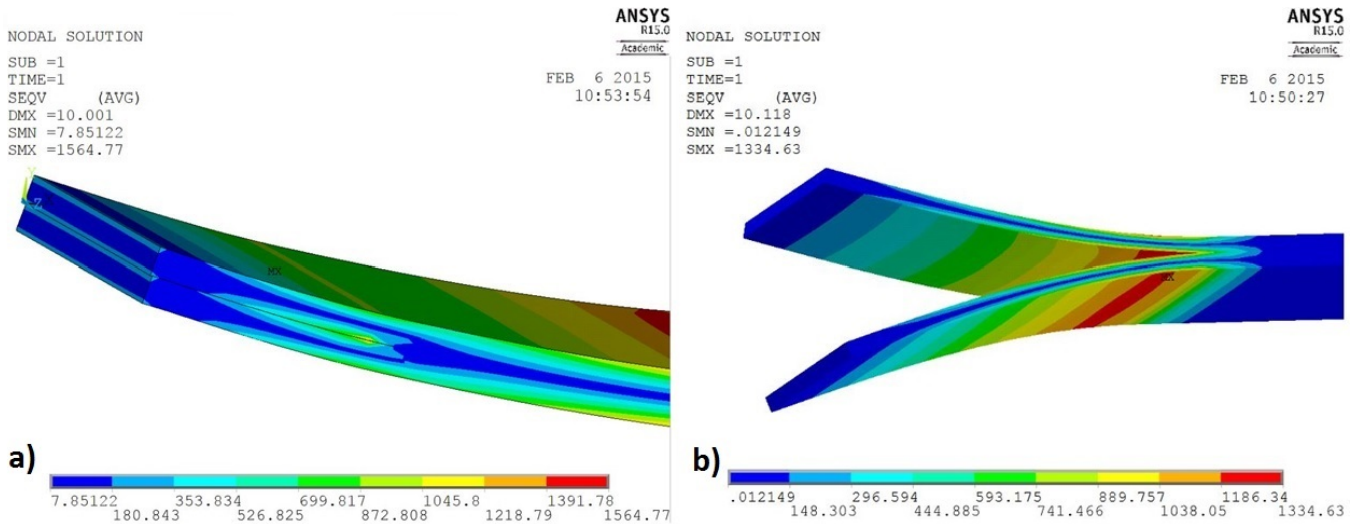


Figure 7. ANSYS model von-Mises stress distribution (N) for (a) ENF and (b) DCB.

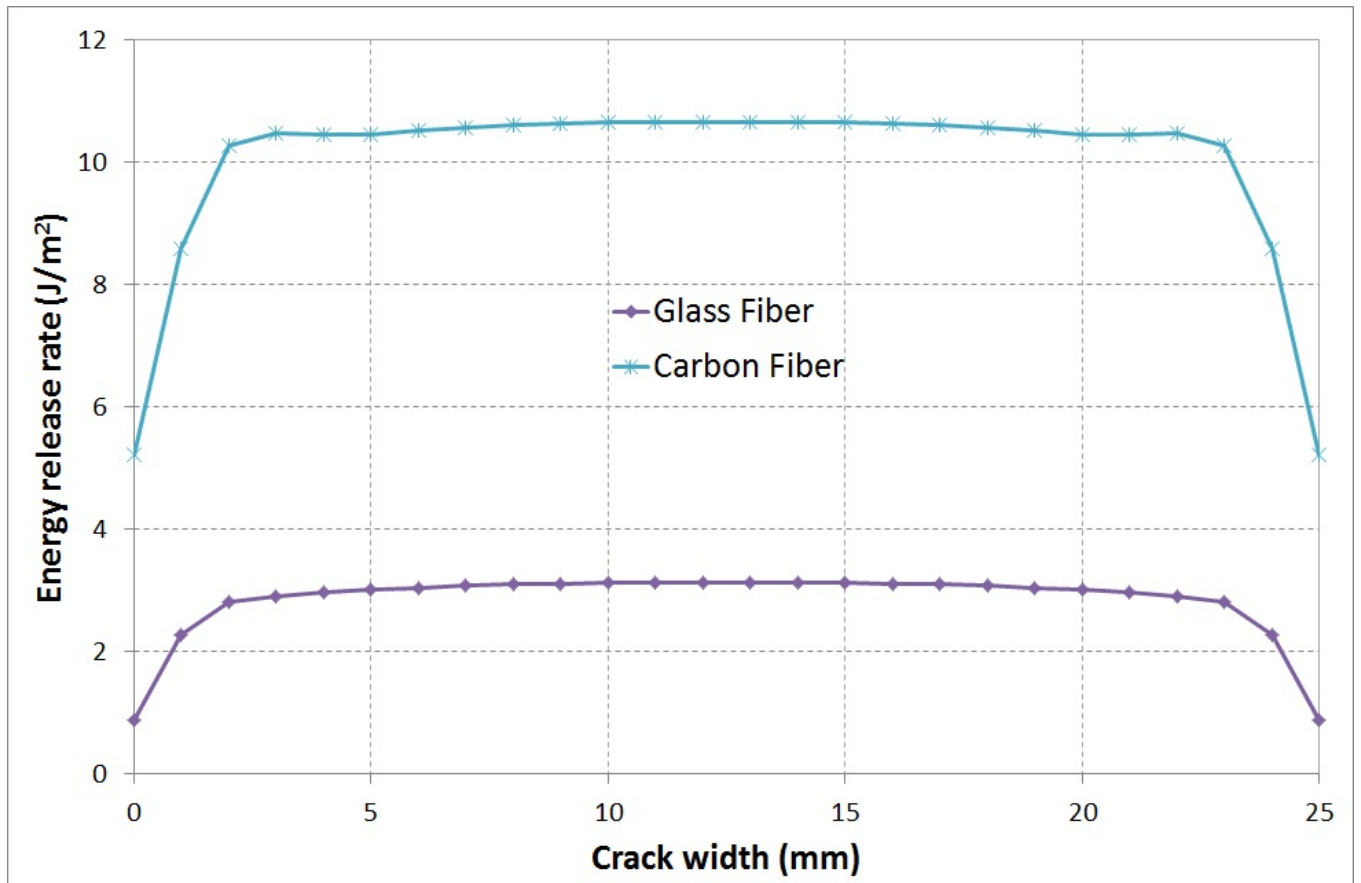


Figure 8. Total energy release rate (Mode-I).

Continued next page.

Continued from previous page.

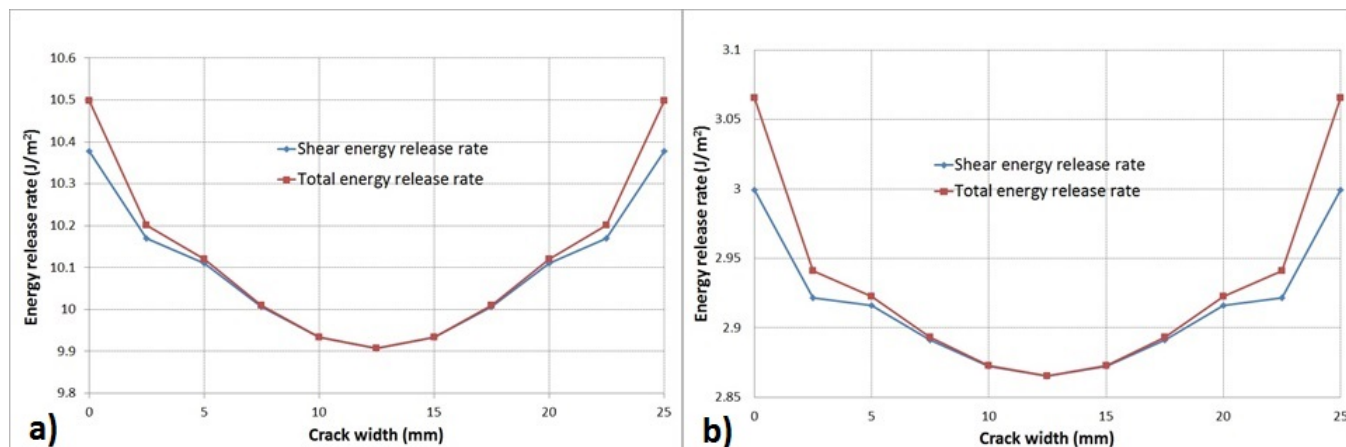


Figure 9. Energy release rates (Mode-II) for (a) carbon fibre and (b) glass fibre.

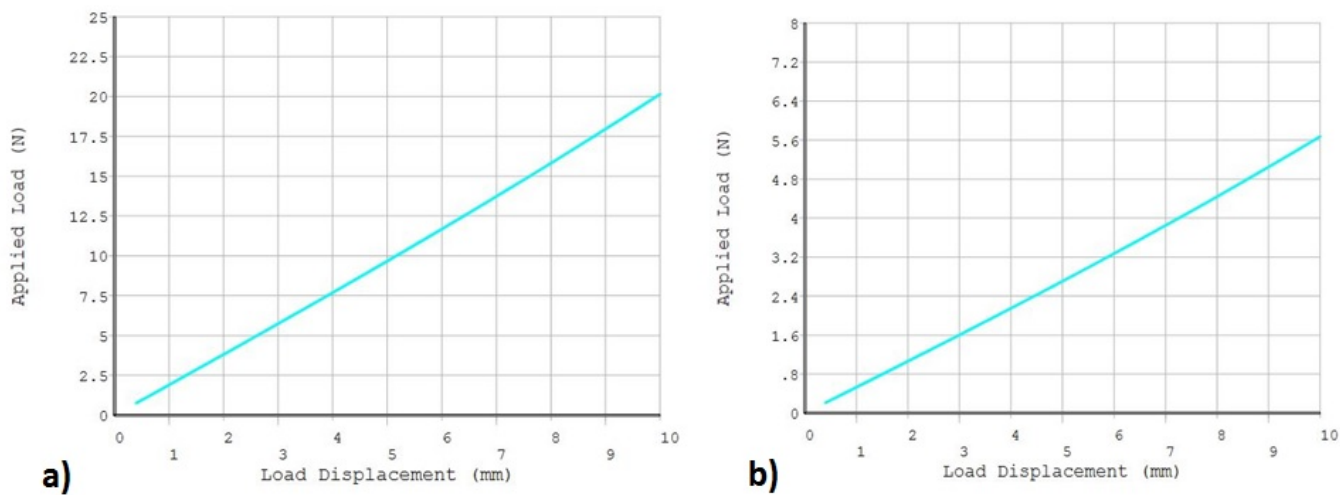


Figure 10. Mode-I DCB testing for (a) carbon fibre and (b) glass fibre.

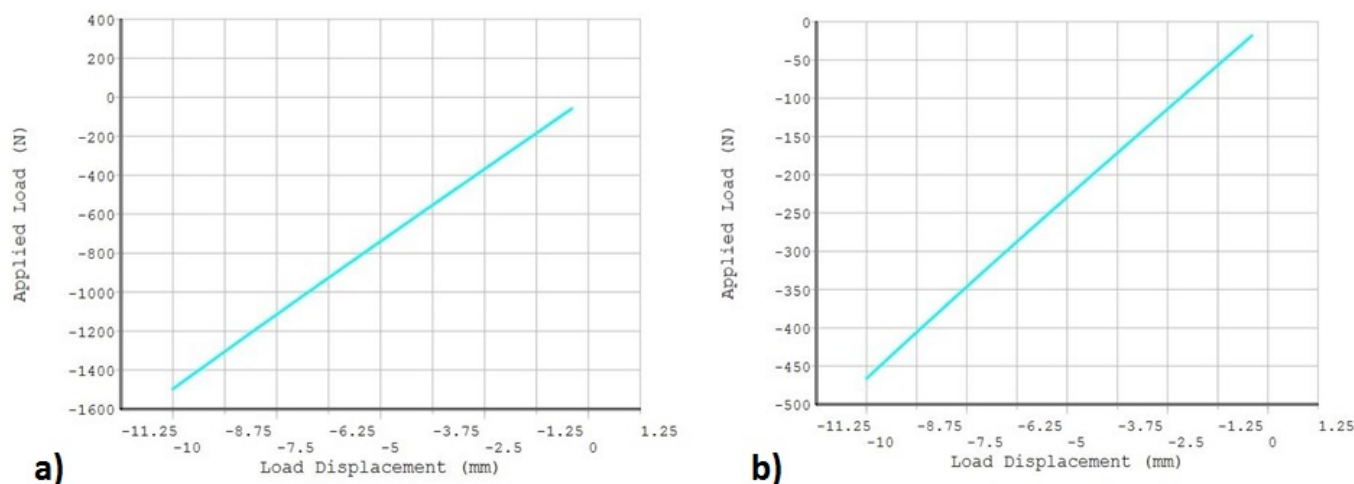


Figure 11. Mode-II ENF testing for (a) carbon fibre and (b) glass fibre.

Continued next page.

Continued from previous page.

## CONCLUSIONS

This paper presents the initial results of a study into the influence of failure on the properties of filament-wound coiled tubes. Numerical simulation was implemented in ANSYS/APDL software to measure the delamination fracture toughness of carbon- and glass-fibre composite laminates. The variation of strain release energy rates versus crack tip in Figures 8 and 9 illustrate that the 2D modelling cannot express the real release strain energy rate at the crack front tip. The contour for  $G_I$  increases—almost doubling in value—from the edge to the centre (from 5 J/m<sup>2</sup> to approximately 10.2 J/m<sup>2</sup>), while  $G_{II}$  slightly decreases from the edge to the centre (from 10.4 to 9.9 J/m<sup>2</sup>). It is, therefore, necessary to investigate the crack propagation in composite laminates using 3D modelling.

According to Figures 10 and 11, the applied load to load displacement perpendicular to the crack plane for carbon fibre is almost three times more than that for glass fibre in Mode-I and Mode-II. The observations are similar to those of Williams (1988) in that the Mode-II interlaminar fracture toughness of composite laminate is several times higher than Mode-I interlaminar fracture toughness in the same material. Also, the DCB testing method (opening mode for normal stress) presents the weakest type of interlaminar delamination failure in composite materials.

## NOMENCLATURE

$\delta$	Load point displacement
$\sigma_{11}$	Normal stress parallel to the fibre direction
$\sigma_{22}$	Normal stress transverse to the fibre-parallel direction
$\sigma_{33}$	Normal stress transverse to the fibre-perpendicular direction
$a$	Crack delamination length
$b$	Sample width
$D_n$	Fatigue damage (equals 0 for $n = 0$ and equals 1 for $n = N$ )
$d_x^u$	Crack displacement in the x direction
$d_y^u$	Crack displacement in the y direction
$E_0$	Initial Young's modulus
$E_f$	Failure Young's modulus
$E_n$	Young's modulus of the material subjected to the $n^{\text{th}}$ cycling loading
$G_I$	Strain energy release rate in Mode-I testing for pure normal stress
$G_{II}$	Strain energy release rate in Mode-II testing for pure shear stress
$G_{III}$	Strain energy release rate in for pure sliding stress
$G_T$	Total strain energy release rate
$2h$	Sample thickness
$N$	Fatigue life
$P$	Load
$R_x$	Node reaction force in the x direction
$R_y$	Node reaction force in the y direction

## ACKNOWLEDGMENTS

The authors would like to express their thanks for the support by the Deep Exploration Technologies Cooperative Research Centre (DET CRC), and Curtin University's Department of Petroleum Engineering. This paper is DET CRC report number 2014/606.

## REFERENCES

- ALFANO, G. AND CRISFIELD, M., 2001—Finite element interface models for the delamination analysis of laminated composites: mechanical and computational issues. *International Journal for Numerical Methods in Engineering*, 50 (7), 1,701–36.
- ANSYS®, 2013—ANSYS Mechanical User's Guide. Release 15.0 Canonsburg, Pennsylvania: ANSYS, Inc.
- BARBERO, E.J., 2013—Finite element analysis of composite materials using ANSYS®. Second edition. Boca Raton, Florida: CRC Press.
- BORDEU, F. AND BOUCARD, P., 2009—A mesoscale model for the prediction of composites materials until final failure. *Proceedings of ICCM-17 17th International Conference on Composite Materials*, 27–31 July, Edinburgh, UK.
- BRUNNER, A., BLACKMAN, B.R.K. AND DAVIES, P., 2008—A status report on delamination resistance testing of polymer-matrix composites. *Engineering Fracture Mechanics*, 75 (9), 2,779–94.
- BURLAYENKO, V.N. AND SADOWSKI, T., 2008—FE modelling of delamination growth in interlaminar fracture specimens. *Budownictwo i Architektura*, 2 (1), 95–109. *Translation: Construction and Architecture Magazine*.
- CHOU PANI, N., 2008—Experimental and numerical investigation of the mixed-mode delamination in Arcan laminated specimens. *Materials Science and Engineering: A*, 478 (1), 229–42.
- DEGRIECK, J. AND VAN PAEPEGEM, W., 2001—Fatigue damage modeling of fiber-reinforced composite materials: review. *Applied Mechanics Reviews*, 54 (4), 279–300.
- GIBSON, R.F., 2011—Principles of composite material mechanics. Third edition. Boca Raton, Florida: CRC press.
- HASHIN, Z., 1980—Failure criteria for unidirectional fiber composites. *Journal of Applied Mechanics*, 47 (2), 329–34.
- JONES, R.M., 1998—Mechanics of composite materials. Second edition. Philadelphia, Pennsylvania: Taylor & Francis, Inc.
- KRUEGER, R., 2004—Virtual crack closure technique: history, approach, and applications. *Applied Mechanics Reviews*, 57 (2), 109–43.
- MATHEWS, M. J. AND SWANSON, S.R., 2007—Characterization of the interlaminar fracture toughness of a laminated carbon/epoxy composite. *Composites Science and Technology*, 67 (7), 1,489–98.
- OCHOA, O.O. AND REDDY, J.N., 1992—Finite element analysis of composite laminates. Dordrecht, The Netherlands: Springer.

Continued next page.

*Continued from previous page.*

PRASAD, M.S., VENKATESHA, C.S. AND JAYARAJU, 2011—Experimental methods of determining fracture toughness of fiber reinforced polymer composites under various loading conditions. *Journal of Minerals and Materials Characterization and Engineering*, 10 (13), 1,263-75.

REIFSNIDER, K., HENNEKE, E.G., STINCHCOMB, W.W. AND DUKE, J.C., 1983—Damage mechanics and NDE of composite laminates. In: Hashin, Z. and Herakovich, C.T. (eds) *Mechanics of Composite Materials: Recent Advances*. New York: Pergamon Press, Inc.

SALEHIZADEH, H. AND SAKA, N., 1992—Crack propagation in rolling line contacts. *Journal of Tribology*, 114 (4), 690-7.

SPADA, A., GIAMBANCO, G. AND RIZZO, P., 2009—Damage and plasticity at the interfaces in composite materials and structures. *Computer Methods in Applied Mechanics and Engineering*, 198 (49), 3,884-901.

SUN, X., TAN, V.B.C., LIU, G. AND TAY, T.E., 2009—An enriched element-failure method (REFM) for delamination analysis of composite structures. *International Journal for Numerical Methods in Engineering*, 79 (6), 639-66.

SZEKRENYES, A., 2002—Overview on the experimental investigations of the fracture toughness in composite materials. *Hungarian Electronic Journal of Sciences. Mechanical Engineering Section*. Document number: MET-020507-A.

THAKUR, V.K., 2013—*Green composites from natural resources*. Boca Raton: Florida. CRC Press.

VAN MIER, J.G.M., 2012—*Concrete fracture: a multiscale approach*. Boca Raton, Florida: CRC Press.

WILLIAMS, J., 1988—On the calculation of energy release rates for cracked laminates. *International Journal of Fracture*, 36 (2), 101-19.

WISHEART, M. AND RICHARDSON, M., 1998—The finite element analysis of impact induced delamination in composite materials using a novel interface element. *Composites Part A: Applied Science and Manufacturing*, 29 (3), 301-13.

WU, F. AND YAO, W., 2010—A fatigue damage model of composite materials. *International Journal of Fatigue*, 32 (1), 134-8.

ZHU, Y., 2009—Characterization of interlaminar fracture toughness of a carbon/epoxy composite material. Master of Science thesis, 15 July 2008. University Park, Pennsylvania: The Pennsylvania State University.

*Authors' biographies next page.*



## THE AUTHORS



**Siamak Mishani** holds a Bachelor of Mechanical Engineering degree and a Master of Science degree in executive management of business administration. He is now undertaking his PhD research at Curtin University's Department of Petroleum Engineering.

Siamak has worked for more than 20 years in—and has in-depth knowledge of—the designing and engineering of coiled tubing and drilling operations. His research aims are to compare the complex stress analyses in composite and steel coiled tubes to improve their mechanical properties under cyclic loading.

*Siamak.Mishani@yahoo.com*



**Vamegh Rasouli** is a Professor in Curtin University's Department of Petroleum Engineering. He is a Chartered Professional Engineer (CPEng) and is a registered engineer with the National Professional Engineers Register (NPER) of Australia. Vamegh received his PhD from Imperial College London in 2002. In 2006, after joining Curtin

University, Vamegh established the Curtin Petroleum Geo-mechanics Group (CPGG), and the Curtin Drilling Research Group (CDRG) in 2010. Vamegh is supervising a number of PhD students and is involved in a number of research and consulting projects in the area of geo-mechanics and drilling. He has undertaken several projects related to petroleum geo-mechanics for various companies, and has also been a consulting engineer on various geo-mechanics-related projects with Schlumberger's Data and Consulting Services (DCS) in Perth.

*v.rasouli@curtin.edu.au*



**Soren Soe** is DET CRC's leader for Project 1.1: Next Generation Drilling Technologies. Soren has held various project, engineering and executive leadership positions since completing his Bachelor of Science degree in engineering in 1991.

He has worked extensively with leading the development of onshore drilling rigs for mineral exploration, production holes, geotechnical applications and coiled tubing rigs for the oil and gas industry.

During his career, Soren has expatriated to China, The Netherlands and Poland with such companies as Knebel Drilling A/S, Boart Longyear and A.P. Moller-Maersk.

*sorensoe@detcrc.com.au*



**Brian Evans** is a Professor in Curtin University's Department of Petroleum Engineering. His background includes graduation as an electrical engineer, mud logger and operations geophysicist, and later as an academic. He helped establish the Department of Exploration Geophysics at Curtin University.

Brian won the 2006 Society of Exploration Geophysicists (SEG) International Distinguished Achievement Award, the 2013 Society of Petroleum Engineers (SPE) International Faculty Award, and the 2014 Subsea Energy Australia (SEA) Business Special Recognition Award. He is the author of the SEG book *A Handbook for Seismic Data Acquisition in Exploration*.

*b.evans@curtin.edu.au*



**Reem Roufail** has a diverse technical background. She earned her BSc and MSc degrees in mechanical engineering from the American University in Cairo, specialising in materials engineering in her BSc degree and material selection for design and failure analysis in her MSc degree.

She joined the mining industry through mineral processing consultants in Canada (G&T Metallurgical Services in Kamloops). Reem then undertook her PhD in mining engineering at the University of British Columbia (titled *The Effect of Stirred Mill Operation on Particles Breakage Mechanism, and their Morphological Features*).

Reem is now working on DET CRC's Project 1.1. Her focus is on selecting the most appropriate coiled tubing material for the coiled tubing drill rig. Her experimental research identifies the strength and bending fatigue resistance of potential coiled tubing materials. She also uses computer numerical analysis to study the distribution of stresses on the coiled tubing in bending.

*Reem.adel92@gmail.com*



**Peter Jaensch** received his BEng degree in mechanical engineering from the University of South Australia in 1997.

Since 1990 Peter has worked for a number of organisations—primarily in research and product development—in fields such as automotive components, special purpose machinery, printing industry new technologies, equine racing equipment, beef abattoir equipment, and mineral exploration drilling equipment.

Peter started with Boart Longyear in June 2010 and he led the engineering team in the development of the LX12 multipurpose drill rig.

Peter has been with DET CRC's Project 1.1 since September 2013 to develop the composite drill to a point where the torsional load and axial load capabilities are adequate for typical drilling operations.

*peter.jaensch@boartlongyear.com*

THIS PAGE LEFT BLANK INTENTIONALLY.